Fungal Biology 125 (2021) 704–717

Contents lists available at ScienceDirect

Fungal Biology

journal homepage: www.elsevier.com/locate/funbio

Transmission of mushroom virus X and the impact of virus infection on the transcriptomes and proteomes of different strains of *Agaricus bisporus*

Eoin O'Connor [a, d], Sean Doyle [a], Aniça Amini [c], Helen Grogan [d], David A. Fitzpatrick [a, b, *]

[a] Department of Biology, Maynooth University, Maynooth, Co. Kildare, Ireland
[b] Kathleen Lonsdale Institute for Human Health Research, Maynooth University, Maynooth, Co. Kildare, Ireland
[c] Sylvan-Somycel (ESSC - Unité 2), ZI SUD, Rue Lavoisier, BP 25, 37130 Langeais, France
[d] Horticulture Development Department, Teagasc Food Research Centre, Ashtown, Dublin 15, D15 KN3K, Ireland

ARTICLE INFO

Article history:
Received 23 September 2020
Received in revised form
8 April 2021
Accepted 21 April 2021
Available online 30 April 2021

Keywords:
Agaricus bisporus
Commercial mushroom
Mushroom virus X (MVX)
Mycovirus
Transcriptomics
Proteomics

ABSTRACT

Cultivation of *Agaricus bisporus* is a large horticultural industry for many countries worldwide, where a single variety is almost grown exclusively. Mushroom virus X (MVX), a complex of multiple positive-sense single stranded RNA (ss(+)RNA) viruses, is a major pathogen of typical *A. bisporus* crops. MVX can manifest a variety of symptoms in crops and is highly infective and difficult to eradicate once established in host mycelium. Currently our knowledge regarding the molecular response of *A. bisporus* fruit bodies to MVX infection is limited. In order to study the response of different *A. bisporus* strains with different susceptibilities to MVX, we designed a model system to evaluate the *in-vitro* transmission of viruses in *A. bisporus* hyphae over a time-course, at two crucial phases in the crop cycle. The symptom expression of MVX in these varieties and the transcriptomic and proteomic response of fruit bodies to MVX-infection were examined. Transmission studies revealed the high potential of MVX to spread to uninfected mycelium yet not into the fruit bodies of certain strains in a crop. MVX affected colour and quality of multiple fruit bodies. Gene expression is significantly altered in all strains and between times of inoculation in the crop. Genes related to stress responses displayed differential expression. Proteomic responses revealed restriction of cellular signalling and vesicle transport in infected fruit bodies. This in-depth analysis examining many factors relevant to MVX infection in different *A. bisporus* strains, will provide key insights into host responses for this commercially important food crop.

1. Introduction

Mushroom virus X (MVX) first appeared in UK *Agaricus bisporus* mushroom crops in 1996. The earliest records noted discrete areas of pinning suppression and bare patches in crops. Initial assumptions were that these symptoms were due to a La France virus infection, but diagnostics revealed completely unrelated double-stranded RNA (dsRNA) elements (Gaze et al., 2000). Empirical evidence pointed to a novel disease, the enigmatic origins and properties of which have resulted in the etymology of 'virus X' (Gaze et al., 2000), a name still used to collectively describe the symptoms observed during infection. Over the next 6 years, MVX became endemic in the UK, the Netherlands, Ireland and other countries with large mushroom industries. Disease phenotypes were inconsistent between countries, with 'bare patches' being more prevalent in the UK and cap browning and discoloration being more common in Ireland, the Netherlands, Belgium and Poland, suggesting geographical symptom variability, and viral composition from different locations (Deakin et al., 2017). The dsRNA profiles of symptomatic mushrooms revealed 26 distinct dsRNA molecules (Grogan et al., 2003). Further research identified significant increases of transcripts, viral in origin, from white, infected, non-symptomatic mushrooms and brown discoloured infected mushrooms (Eastwood et al., 2015). A link between viral load and the extent of browning in infected mushrooms was also observed (Eastwood et al., 2015). It is now understood that MVX represents multiple viruses in a virus complex or virome of *A. bisporus*. Next Generation Sequencing (NGS) techniques shed new insight on the

* Corresponding author. Genome Evolution Laboratory, Department of Biology, Maynooth University, Maynooth, Co. Kildare, Ireland.
E-mail address: david.fitzpatrick@mu.ie (D.A. Fitzpatrick).

https://doi.org/10.1016/j.funbio.2021.04.005

List of abbreviations

CEM	Compost extract media
Ctrl	non-infected mushrooms
CYM	Complete yeast media
CWH	Commercial-Wild Hybrid
DEGs	Differentially expressed genes
dsRNA	Double-stranded RNA
DTT	Dithiothreitol
FISH	fluorescence in situ hybridisation
GO	Gene Ontology
IAA	Iodoacetamide
LC-MS/MS	Liquid chromatography mass spectrometry
NGS	Next generation sequencing
MC	Late infection
MS	Early infection
MVX	Mushroom virus X
OWC	Off-White Commercial
SCC	Smooth Cap Commercial
ssDNA	Single stranded DNA
ss(+)RNA	Positive-sense single stranded RNA
TCA	Trichloroacetic acid
TFA	Trifluoroacetic acid

characterisation of the virus within the MVX complex including, the taxonomic distribution of viruses, viral genome composition, the number of individual viruses and the discrete RNAs they consist of Deakin et al., (2017). Furthermore, the AbV16 virus, causal for the brown cap disease phenotype, was shown to be a multipartite virus consisting of four segments of RNA while the AbV6 virus, which is more associated with the bare patch phenotype, is a bipartite segmented virus composed of two RNAs (Deakin et al., 2017). Eighteen individual viruses are now known to belong to the MVX complex spanning a range of taxonomic families including Benyviridae (ss(+)RNA viruses of plants (Gilmer and Ratti 2017), Narniviridae (mycovirus), Hypoviridae (mycovirus (Suzuki et al., 2018)), the order Tymovirales (ss(+)RNA primarily viruses of plant) and the new virus family, Ambsetviridae (Deakin et al., 2017). The dynamism of the MVX complex and constituent viruses along with their disparate homologies to different phylogenetic sources is suggestive of multiple ancient infection events into wild populations of *Agaricus* (Deakin et al., 2017). Viruses have previously been identified in other edible mushrooms such as a dsRNA virus in *Flammulina velutipes* (Magae and Sunagawa 2010), a dsRNA virus in *Lentinula edodes* (Magae 2012; Kim et al., 2013), a ss(+)RNA virus in *Pleurotus ostreatus* (Kim et al., 2008) as well as other fungi such as a single stranded DNA (ssDNA) virus of the phytopathogenic fungus *Sclerotinia sclerotiorum* (Yu et al., 2010).

MVX first appeared during a period of technological advancement in many major *A. bisporus* cultivating countries, namely, the adoption of bulk phase III compost. Phase III compost consists of pasteurised phase II compost that is fully colonised with *A. bisporus* mycelium in large, environmentally-controlled purpose built tunnels. Prior to being filled into growing rooms, the fully colonised phase III compost must be removed from the tunnel and broken apart for transportation. This process leads to massive breakages of the mycelium, which triggers rapid repair by new growth and anastomosis (hyphal fusion). This process of breaking apart the mycelium within the phase III compost and transporting it via conveyors and trucks to growing rooms leaves it very vulnerable to infection, particularly from any MVX-infected mycelium that may contaminate it. The re-anastomosing of the mycelial mass within the bulk phase III compost that follows will facilitate the transmission and replication of MVX, as hyphae are more exposed, temporarily damaged (stress), and cell division and anastomis is greatly increased (Eastwood et al., 2015).

The mushroom industry contends with a great variety of crop pathogens from fungi, bacteria, invertebrates and viruses. One of the causes for the persistence of certain pathogens and the ease of spread of novel diseases from farm-to-farm, is due in part to the lack of genetic variation in the mushroom strains used in commercial cultivation. A single *A. bisporus* variety has dominated the commercial *Agaricus* industry for decades, resulting in what is essentially a monoculture crop. The lack of new varieties being introduced to the mushroom market is due in part to difficulties in breeding arising from the life cycle of *A. bisporus* (Sonnenberg et al., 2017). The use of novel hybrids and wild isolates of *A. bisporus* in breeding programmes would be desirable to provide genetic diversity that could introduce some degree of resistance or tolerance to pathogens and reduce their impact on the crop. Off-white and brown varieties (wild) have already been shown to have heightened resistance to mycovirus infection, likely through vegetative incompatibility with commercial white strains. The work described in this paper tests the hypothesis that genetically diverse strains of *A. bisporus* are less susceptible to MVX. We use a range of *A. bisporus* strains to understand susceptibility to MVX, degree of resistance, symptom expression in infected crops as well as the transcriptomic and proteomic response of *A. bisporus* strains to MVX infection. Results from this work will elucidate host responses upon exposure to MVX and elucidating the *A. bisporus* virus interaction will add to the knowledge base of breeders in their quest to generate potential MVX-resistant strains.

2. Methods

2.1. Strains and culture conditions

Five strains of *A. bisporus* were used for this study, with the exception of the transcriptomic work where three strains were selected from the five. The three strains used in every aspect of this study included: the most widely used contemporary commercial strain A15 (derived from Horst U1), a novel hybrid strain with commercial (Horst U1) and wild strain parentage denoted as commercial-wild hybrid (CWH), and a wild strain from the *Agaricus* resource program known as ARP23 used in commercial breeding. The remaining two strains were earlier commercial hybrid strains that are still used in commercial breeding; a smooth cap commercial hybrid (SCC, Somycel 53) and an off-white commercial hybrid (OWC, Somycel 76).

The MVX-infected culture MVX-1153 was isolated from *A. bisporus* A15 mushrooms presenting brown-cap disease phenotype from an Irish mushroom farm in July 2016. Small sections of internal mushroom cap tissue (2–3 mm) were aseptically cut from diseased mushrooms and cultured on compost extract media (CEM) for 2 weeks at 25 °C in the dark. To make compost-based inoculum, 30 g of phase II compost was autoclaved in 250 ml Duran flasks at 121 °C for 1 h and repeat autoclaved after 24 h to eradicate endospores. When cool, 3–6 × 5 mm plugs of MVX-1153 culture were added and incubated for 3 weeks at 25 °C in the dark. Compost colonised with MVX-infected mycelium was used as an inoculum for all cropping experiments.

2.2. In-vitro *MVX-transmission protocol*

Dual-culture interactions were set up to assess the *in-vitro* transmission potential of MVX from an MVX-infected donor strain to a non-infected recipient strain over a time-course. MVX-1153 was isolated from an A15 commercial crop and so exhibits full vegetative compatibility with A15. Agar plugs containing hyphae from the donor and recipient strains were placed 10 mm apart on CEM and incubated at 25 °C ($n = 3$). Cultures were monitored during initial colony growth and the first time-point (T_0) hyphae were extracted when the donor and recipient strains made contact (this was after 3 days for all dual-culture interactions). T_1 hyphae were collected 6 days after T_0 and T_2 hyphae were taken 12 days after T_0. Time-point hyphae were excised as two agar plugs (7 mm Ø) from the top and bottom outer periphery of the growing edge of donor and recipient cultures (Fig. 1A) and were sub-cultured onto Petri dishes of complete yeast medium (CYM) coated with a 90 mm disc of sterile cellophane (CYM: 2 g proteose peptone, 2 g yeast extract, 20 g glucose, 0.5 g $MgSO_4$, 0.46 g KH_2PO_4, 1 g K_2HPO_4, 20 g agar in 1 l dH_2O) Sub-cultures were incubated at 25 °C in the dark for 3 weeks after which mycelium was carefully removed from the cellophane, flash-frozen, freeze-dried and stored at −80 °C for subsequent MVX diagnostics.

2.3. *Cropping experiment*

A semi-commercial cropping experiment was set up to assess the transmission potential of MVX-1153 at two different infection times with the five strains of *A. bisporus*; A15, CWH, ARP23, SCC and OWC, respectively. The three treatments used for each strain were; MVX-1153 inoculation at the beginning of spawn run (MS; early infection), MVX-1153 inoculation at the beginning of case run (MC; late infection), and control uninfected plots. Treatments are described in detail below. Each treatment ($n = 3$) for each strain ($n = 5$) was prepared in triplicate ($n = 3$). Mushroom spawn for strain A15 was provided by Sylvan. Mushroom spawn for the remaining strains was prepared by adding 180 g of cooked and sterilised rye grain (provided by Sylvan) to 500 ml Duran flasks and autoclaving for 1 h to ensure sterility. For each strain, 6 × 5 mm agar plugs were added to the sterilised grain and incubated at 25 °C for four weeks in the dark, with gentle agitation of the flasks once a week to ensure good colonisation of the rye grains. One jar of spawn was prepared for each replicate (9 jars in total for each strain). Nine x 180 g jars of A15 spawn were also prepared. All spawn was stored at 4 °C degrees until needed.

Cropping was carried out as per industry standards in an environmentally controlled mushroom growing unit (Fancom 765 computer system). One jar of *Agaricus* spawn (180 g) was added and gently mixed throughout 18 Kg of pasteurised phase II mushroom compost at a rate of 1.0% for each plot, which was then used to fill pre-cleaned and steamed polypropylene crates (0.6 × 0.4 × 0.24 m, 45 L). The first infection treatment (MS) was carried out at this point by addition of MVX-1153 compost inoculum at a rate of 0.01% to the assigned plots. This was done by leaving approximately 50 mm of the plot unfilled, sprinkling MVX-1153 compost fragments evenly on the surface and continuing to fill to the final weight of 18 Kg. Plots were incubated (spawn run) at 25 °C, 90–95% RH, with recirculated air with high levels of ambient CO_2 (>6000 ppm) for 17 d to allow for full colonisation of compost with *A. bisporus* mycelium. The second infection treatment (MC) was

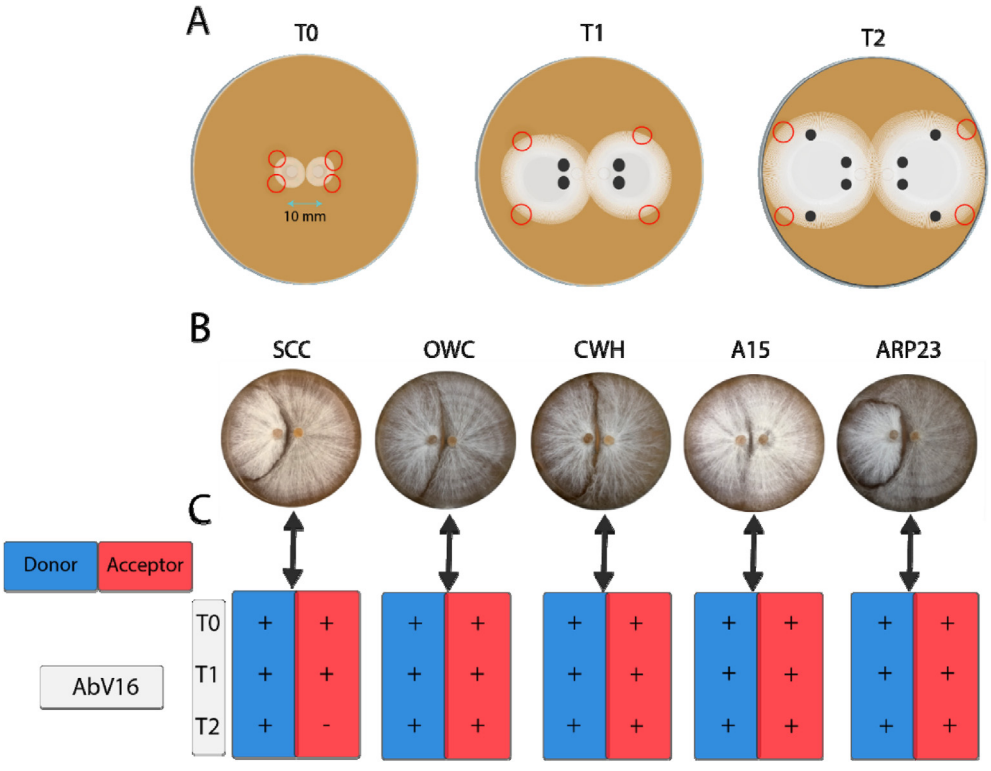

Fig. 1. Overview of experimental design and main finding of *in vitro* MVX transmission experiment. (A) Culture setup and sample collection over three time-points. Red circles indicate areas where samples are taken for subsequent MVX diagnostics. Agar plugs from donor strain (MVX 1153) and acceptor strain (non-infected) are placed 10 mm apart. Samples are taken at the first day of anastomosis (T_0), 6 days after (T_1) and 12 days after (T_2). (B) Images of the five interactions. Headers for each plate indicate the acceptor partner, where the donor is on the left and the acceptor is on the right. Note the variety of interactions between all crossing cultures. (C) Indicates either a positive (+) or negative (−) diagnostic for AbV16 ($n = 3$). (For interpretation of the references to colour in this figure legend, the reader is referred to the Web version of this article.)

added at this point to the assigned plots using the same method described for the MS treatment: (approximately 50 mm of colonised substrate was gently removed, the MVX-1153 compost inoculum was sprinkled over the surface and the colonised substrate was replaced). Plots were then covered with 50 mm of pre-wetted peat-based 'casing' soil (Harte Peat, Clones, Co. Monaghan, Ireland). Plots were incubated under the same conditions for an additional 7 d to allow for mycelium from the compost layer to grow into the casing layer. At this point, temperature and humidity were lowered steadily over a 3 d period from 25 °C to 18 °C and 90–95% RH to 85–90% RH and CO_2 levels were lowered by introducing filtered fresh air into the air handling system. These environmental conditions were maintained to allow for primordia initiation ('pinning') and ultimate mushroom formation. Mushrooms were harvested 17–21 d (1st flush) and 24–28 d (2nd flush) after casing. A representative symptomatic mushroom with visible MVX phenotype (when available) from each plot was picked from both flushes. Mushrooms were immediately flash-frozen, freeze-dried and stored at −80 °C for subsequent molecular analyses. All other mushrooms were weighed to record yield.

2.4. Colour measurements

Data on mushroom colour was collected for every mushroom picked over two harvests (flushes). Colour measurements were recorded with a Minolta CR-400 chroma meter (Konica Minolta Inc., UK; illuminant D65, measurement aperture area ø = 8 mm). Measurements were taken in accordance to the CIE L*a*b* colour space. Calibrations were made using a white calibration plate (CR-A43) prior to colour recordings. A colour distance differential (ΔE) was calculated for each mushroom (Fleming-Archibald et al., 2015). Statistical significance quoted within the treatments of each strain are based on single factor ANOVA ($P < 0.05$). Differences between first and second flush were made in relation to the differences observed between mushroom controls and mushroom treatments within the same flush.

2.5. Diagnostics of disease-associated viruses AbV6 and AbV16

MVX diagnostics was performed on mycelium from dual-culture transmission experiments and fruit bodies from the different treatments and controls. All the mycelium from culture plates was used and 100 mg of fruit body material was used. dsRNA isolation, CF11 column purification, Super-Script® VILO™ cDNA synthesis and PCR amplification of AbV16, AbV6 and GPD II (quality control) cDNAs were performed as previously described (Fleming-Archibald et al., 2015).

2.6. RNA isolation, sequencing and data processing

RNA sequencing was carried out on mushroom samples for strains A15, CWH and ARP23 to assess changes in gene expression in fruit-bodies derived from mycelium exposed to MVX at two inoculation timepoints (MS and MC). Triplicate mushroom samples from the 1st flush were used for the three strains and two infection times. The freeze-dried mushroom samples were crushed in liquid N_2. RNA was isolated using the RNeasy plant minikit (Qiagen) as per the manufacturer's guidelines. DNA digestion was done with DNase I (Invitrogen). RNA quantity and quality was assessed with an RNA6000 Nano Assay (Agilent 2100 Bioanalyzer, Agilent Technologies, USA). High-purity RNA isolations (RIN ≥ 8.5) were sent to BGI Tech Solutions Co., Ltd. (Hong Kong, China) for cDNA library construction and RNA sequencing (BGISEQ-500, PE100). Paired-end reads (100 nt) from each sample ($n = 27$) were filtered to remove low-quality regions (phred score < 20) and artefactual adaptors were removed with Cutadapt (Martin 2011). Trimmed reads were aligned to the genome of *A. bisporus* var. *bisporus* (H97) v2.0 (Morin et al., 2012) using Hisat2 (Kim et al., 2015). Transcripts were quantified using Salmon (Patro et al., 2017). Transcript counts were normalised and significantly differentially expressed genes (DEGs) were assessed between samples using DESEQ2 (Love et al., 2014). DEGs were filtered by significance ($P < 0.05$) and a liberal $\log_2$ fold change greater than or less than ± 1.5.

2.7. Whole cell lysate protein extraction and LC-MS/MS analyses

Proteomic analyses were carried out on mushrooms of all five strains. For protein extractions 100 mg of starting material was used. Freeze-dried samples were crushed in liquid N_2. Ground material was added to a lysis buffer (100 mM Tris–HCl, 50 mM NaCl, 20 mM EDTA, 10%(v/v) glycerol, 1 mM PMSF and 1 μg ml^{-1} Pepstatin A pH 7.5) and subjected to sonication (Bandelin Sonoplus HD2200, Bandelin Elec.) three times, with a 1 min incubation on ice between each round. Cell lysates were centrifuged at 20,200×*g* for 10 min (4 °C) twice until clarified and brought to 15% (w/v) trichloroacetic acid (TCA) with additional acetone for precipitation. Proteins were resuspended in 6 M urea, 2 M thiourea and 100 mM Tris–HCl pH 8.0 and then adjusted to 1 M urea with addition of ammonium bicarbonate. 15 μg of protein for each protein lysate preparation was reduced using 65 mM dithiothreitol (DTT), alkylated using 55 μL of 1 M iodoacetamide (IAA) per millilitre of lysate, and digested using a combination of sequencing-grade trypsin and ProteaseMAX surfactant at a concentration of 0.01% (w/v) (O'Keeffe et al., 2014). Digested peptides were acidified with addition of trifluoroacetic acid (TFA). C_{18} ZipTips ((Millipore® Ziptips C18)) were used to desalt 5 μg of tryptic peptides for Mass spectrometry. 750 ng of peptide mix was eluted onto a Q-Exactive (ThermoFisher Scientific, U.S.A) coupled to a Dionex RSLCnano for analysis by nano-flow liquid chromatography electro-spray ionisation tandem mass spectrometry (LC-MS/MS). LC gradients from 3 to 45% B were run over 110 min and data and the Top15 method used to collect data for MS/MS scans. Spectra were sorted into polypeptides by alignment to the predicted protein database of *A. bisporus* var. *bisporus* (H97) v2.0 (Morin et al., 2012). MaxQuant (version 1.6.2.3) with integrated Andromeda used for database searching (Cox and Mann 2008). MaxQuant parameters are as previously described (Owens et al., 2015). Removal of reverse hits and contaminant sequences, filtering of protein hits found in only a single replicate ($n = 3$), and Log_2 transformation of LFQ intensities was performed using Perseus (version 1.4.1.3 (Tyanova et al., 2016)).

2.8. Functional annotation of transcriptomic and proteomic data

Transcriptomic and proteomic data were functionally annotated using BLAST2GO (version 5.2.4; Conesa et al., 2005; Gotz et al., 2008). Sequences were queried against the NCBInr database using BLASTp (E value hit filter E^{-03}) and EMBL-EBI database using InterProScan (Altschul et al., 1997; Jones et al., 2014). The CloudIPS resource was utilised for the most up-to-date databases in the dedicated computing cloud (2019.09). Independent InterproScan 5 searches were employed in parallel to assign Pfam IDs and associated Gene Ontology (GO) Term IDs. Predicted proteins were subjected to the complete GO workflow in BLAST2GO (GO cut off 55, GO weight 5, E value hit filter E^{-06} and default computational evidence codes). Significantly enriched terms were assigned using a Fisher's exact test ($P < 0.05$). All gene accession IDs listed in this text

are preceded by the Joint Genome Institute (JGI) identifier 'jgi|Agabi_varbisH97_2'.

3. Results

3.1. In vitro *horizontal transfer of MVX*

MVX is hypothesised to primarily transfer from an infected host mycelium to non-infected hyphae via horizontal transmission (hyphal anastomosis). The transmission potential of MVX was trialled in dual-culture interactions whereby a donor (MX-1153) and acceptor (five strains of *A. bisporus*) cultures were grown together to facilitate potential transfer of viruses. Diagnostics were conducted for AbV16 (the virus linked to the brown cap disease-phenotype) at three time-points (T_0-T_2) in triplicate (Fig. 1C). A total of 90 MVX assays were conducted. No AbV16 virus-loss was noted in any of the donor hyphae as positive diagnostics for AbV16 were recorded for all time-points. Acceptor hyphae in all five strains were positive for AbV16 as early as T_0 (first day of anastomosis). Temporal findings for the detection of AbV16 were also positive in T_1 and T_2, except for SCC T_2. No detection of AbV6 was recorded in any donor or acceptor strain in any time-points. The lack of AbV6 in both donor and acceptor hyphae is expected, as the source inoculum MVX-1153 did not test positive for this virus when originally sampled (not shown). Our results show that a variety of interactions can occur between the donor and acceptor strains (Fig. 1B). The MVX-1153 donor and A15 acceptor dual culture display the highest level of interaction where the two cultures meet, compared to other pairings where the interaction zones have much reduced hyphal interactions between the cultures but this is unsurprising as MVX-1153 and A15 are vegetatively compatible strains. These findings show that the AbV16 virus can horizontally transfer from an infected mycelium to all five strains *in vitro*, even at different levels of vegetative compatibility, once an interaction zone has been established.

3.2. *MVX diagnostics in fruit bodies of five strains of* A. bisporus

RT-PCR tests for the presence of MVX were also undertaken on the fruit bodies of each of the five strains and corresponding treatment (Fig. 2). The same culture used in the *in vitro* dual-culture interactions (MVX-1153) was used to infect plots in the *in vivo* cropping experiment at either an early (MS) or later (MC) stage in the crop cycle. Our results show that for the early infection (MS) plots, the A15 strain had a positive test for two of the three fruit bodies tested, the highest incidence for any strain tested (Fig. 2). Conversely, AbV16 was not detected in MS treatments for strains SCC, OWC and ARP23. The only other strain with detection at MS was CWH ($n = 1/3$; Fig. 2).

A different pattern was observed for the late infection (MC) plots. AbV16 was detected in all samples of A15 ($n = 3$). All other strains, bar CWH, tested positive for the AbV16 band in one MC replicate. In terms of infectivity, MC treatments produced the highest level of AbV16 detection (Fig. 2). CWH was the only strain that tested negative in each replicate for AbV16. CWH cannot be considered totally MVX-resistant as AbV16 was detected in one MS replicate (Fig. 2).

We also tested for the presence of AbV6 in all strains and corresponding treatment time points (Fig. 2). AbV6 was not present in the initial MVX-1153 inoculum and so AbV6-infection was not anticipated in any fruit body for MS or MC treatments. As expected, no AbV6 was recorded in strains SCC, OWC, CWH or A15 (Fig. 2). However, AbV6 was detected in a single MS and MC replicate for strain ARP23 (Fig. 2).

3.3. *Mushroom colour measurements from the cropping experiment*

The impact of MVX-inoculation on mushroom cap colour was assessed through chromometric analyses of fruit bodies following MS and MC treatments in all five strains. A prominent symptom of MVX is varying degrees of cap discolouration from off-white to distinct shades of brown (Fig. 3). 'Whiteness' was evaluated by measuring ΔE of each mushroom, the lower the ΔE, the whiter the mushroom. A total of 1050 mushrooms and 2460 fruit bodies were measured for ΔE in first and second flush, respectively. An overall trend is seen in all five strains whereby the introduction of MVX inoculum at MS and MC results in higher ΔE values (Fig. 4). The mean ΔE in all strains is higher in MS and MC treatments compared to controls. Whiteness seems least affected in strain SCC, where mean ΔE values are very similar. Some high ΔE outliers can be seen in the 1st flush MC treatment and 2nd flush MS treatment, but these values do not result in any significant differences between controls and treatments (ANOVA, $P < 0.05$). Average ΔE for strain OCW MS and MC are both significantly higher than the controls in the 1st and 2nd flushes. A similar trend is also seen for the CWH MS and MC treatments but the average ΔE values for the later MC treatment are also significantly higher than the earlier MS treatment in both flushes. Strain A15 also had significantly higher ΔE values in 1st and 2nd flush for both MS and MC treatments compared to the uninoculated control, however, MS and MC were not significantly different to one another in either flush. Interestingly, the naturally-brown coloured ARP23 showed significantly greater ΔE values in both flushes following both the early and late MS and MC treatments compared to controls, where MC had a higher mean in the 1st flush and MS higher in the 2nd flush. In terms of overall frequency of increased ΔE values related to MVX-infection, the 2nd flush appears to be more impacted than the 1st flush for most strains (Fig. 4). In general the differences between the early (MS) and later (MC) infection timings are not significant apart from strains CWH and ARP23.

3.4. *MVX disease phenotypes and mushroom yield*

Different disease phenotypes were noted in the experimental crop (Fig. 3A–D). The off-coloured/brownish fruit bodies was the most prevalent of the phenotypes (Fig. 3A–B). Thickened/misshapen stipes were noted in MVX-inoculated plots of A15 (Fig. 3C), a phenotype previously recorded in diseased crops (Grogan et al., 2003). Unlike the other four strains, CWH displayed premature cap-opening of mushrooms from MVX-inoculated plots (32 incidences) (Fig. 3D). There was a significant difference ($P < 0.001$) in the average yield across all treatments between all strains in the order CWH > A15 > OWC > ARP23 > SCC (Fig. 3E and Table S1). MVX 1153 inoculation also significantly increased yield across all strains ($P < 0.05$) in the order MC > MS > Control although OWC did not appear to reflect this trend (Fig. 3E). Although some strains appeared to respond differently to inoculation there was no significant interaction effect ($P = 0.21$) (Fig. 3E).

3.5. *Overview of the transcriptomic response of strains A15, ARP23 and CWH to MVX-inoculation*

Out of the five *A. bisporus* strains in this work, strains A15, CWH and ARP23 were chosen for transcriptomic analyses. Comparisons of early MVX-inoculation (MS) and late MVX-inoculation (MC) to non-infected (Ctrl) mushrooms were made to compare levels of differentially expressed genes (DEGs) between each strain. A full list of DEGs for each strain and treatment timepoint can be found in supplementary information (Table S2).

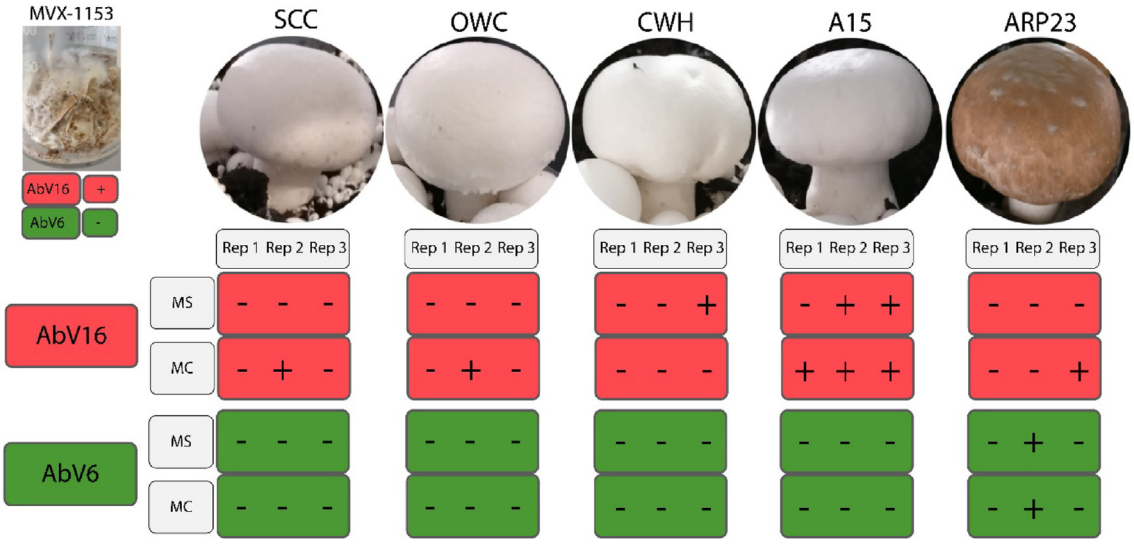

Fig. 2. MVX diagnostics (RT-PCR) from the cropping experiment. Images of fruit bodies correspond to control treatments. MVX-1153 was introduced at the beginning of spawn run (MS) and beginning of case run (MC) to the compost layer of individual plots (+: band present, −: band absent). Control mushrooms were all negative for both AbV16 and AbV6 (not shown).

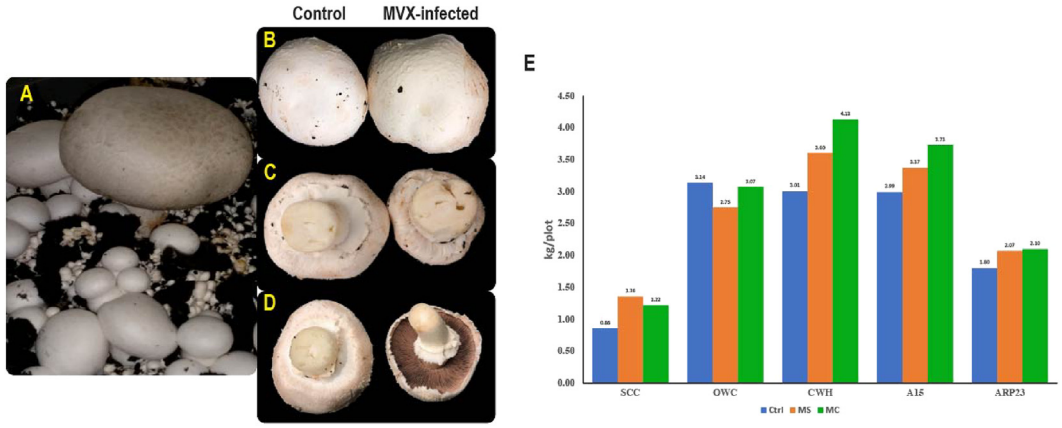

Fig. 3. MVX disease phenotypes manifested in the experimental crop and impact on fruit body yield. (A) An off coloured 'brown' mushroom growing next to white mushrooms in an MVX-infected plot. (B) A white control mushroom compared to an irregularly shaped off-white mushroom from an MVX-infected plot. (C) Comparison of a control mushroom stalk next to an enlarged/swollen stalk of a mushroom from an MVX-infected plot. (D) Comparisons of medium sized mushrooms, where the control mushroom is a high-quality closed-cup and the mushroom from an MVX-infected plot has a prematurely opened cap. (E) Comparison of average yield of fruit body biomass (kg/plot) between each strain and treatment. (For interpretation of the references to colour in this figure legend, the reader is referred to the Web version of this article.)

3.5.1. A15 transcriptomic response

Looking at the A15 MS exposure to MVX our results show that 304 genes were upregulated and 15 were downregulated relative to the control (Table S2). With respect to the A15 MC treatment, 103 genes were upregulated and 44 were downregulated. In terms of a shared response to MVX both A15 MS and MC treatments share 84 upregulated genes including a cutinase gene (accession:183005), a nuclear envelope stress response gene (accession:187933) and a late embryogenesis abundant gene (accession:178286) (Table S2). They also share 6 downregulated genes all with unknown functions bar a Prolyl oligopeptidase (accession:219134) (Table S2).

In terms of DEGs in the A15 MS and MC treatments. Many common GO terms are overrepresented in the upregulated DEG list, including reproduction (GO:0000003), metabolic processes (GO:0008152), cellular processes (GO:0009987), cell (GO:0005623), protein-containing complex (GO:0032991), organelle (GO:0043226), cell part (GO:0044464), catalytic activity (GO:0003824), and structural molecule activity (GO:0005198) (Table S3). In terms of the downregulated genes, the list of common GO terms between MS and MC treatments includes transporter activity (GO:0005215) and transmembrane transporter activity (GO:0022857). Interestingly cellular component organization (GO:0071840) and binding (GO:0005488) are overrepresented in the downregulated MS treatment but overrepresented in the upregulated list of MC treatment (Table S3).

3.5.2. CWH transcriptomic response

The CWH MS treatment displayed 46 upregulated and 48 downregulated genes with respect to the control, while 64 upregulated and 4 downregulated genes where observed in the CWH MC treatment relative to the control. The number of shared genes between both CWH treatments was relatively low however, with only 7 upregulated genes being observed in both treatment time points, Most genes had no putative functions but a gene with transcription factor activity (accession:138736) was noted. Only a

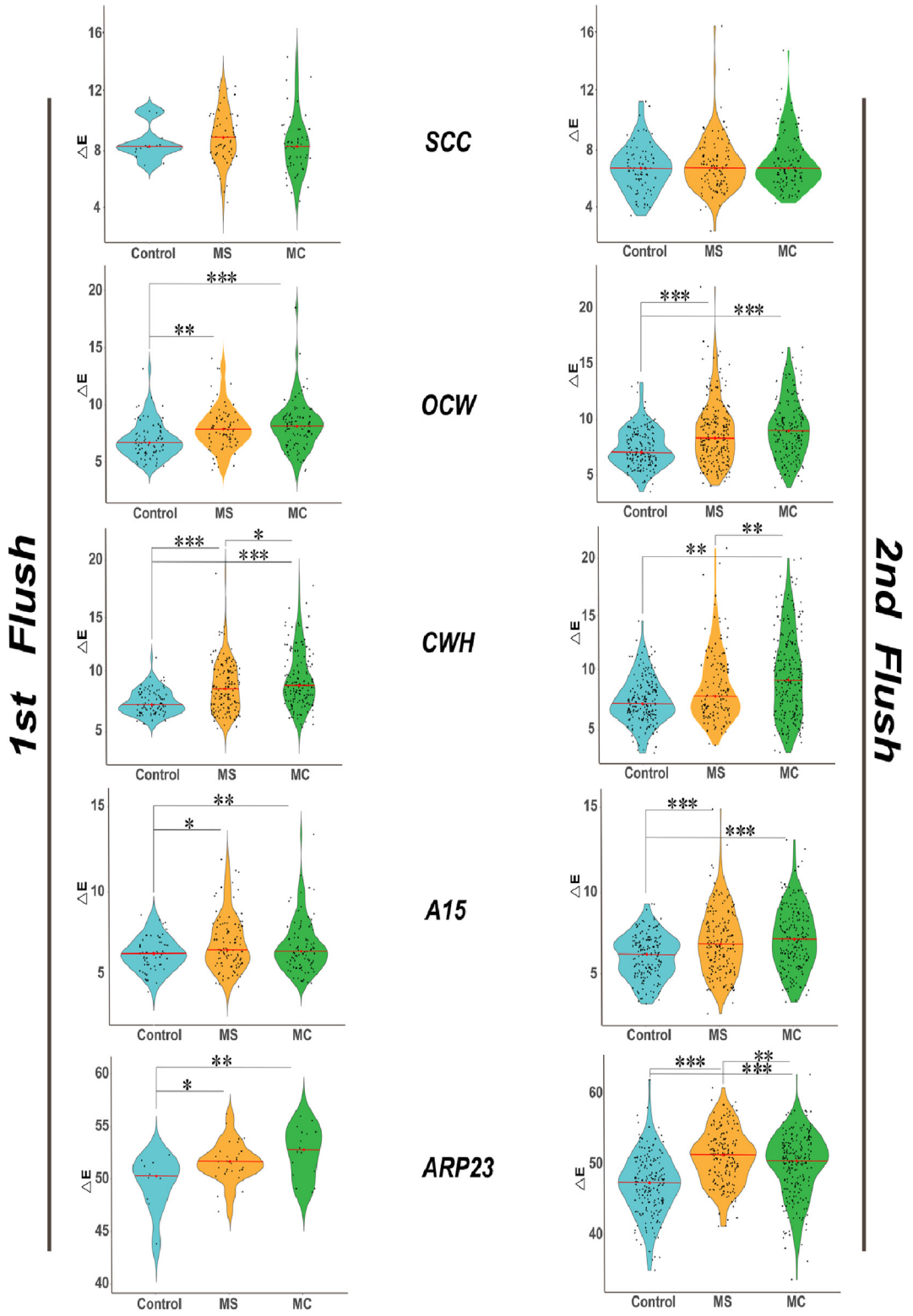

Fig. 4. Chromo metric data for 1st **and 2**nd **flush mushrooms from MVX-infected experimental crop.** Violin plot used to compare disparity of colour data (ΔE) of control treatments to MVX-inoculated plots in the first and second flush. Low ΔE values of <10 are representative of good quality white mushrooms. Mean values are represented by a red line. The width of the plot represents frequency/clustering of colour data to a given ΔE reading. Significant differences were observed between MVX-inoculation at spawning (MS) and MVX-inoculation at casing (MC) treatments (*: $P < 0.05$, **: $P < 10^{-3}$, ***: $P < 10^{-5}$). (For interpretation of the references to colour in this figure legend, the reader is referred to the Web version of this article.)

single downregulated gene for a sugar transporter (accession: 183903) was observed between both CWH treatments (Table S2).

In terms of DEGs in the CWH MS and MC treatments. Only two common GO terms are overrepresented in the upregulated DEG list, these are for catalytic activity (GO:0003824) and small molecule metabolism (GO:0044281) (Table S3). In terms of the downregulated genes, no common GO terms are observed (Table S3).

3.5.3. ARP23 transcriptomic response

The ARP23 MS treatment resulted in 108 genes being upregulated and 302 downregulated with respect to the control while a reduced response was observed in the MC treatment with only 14 genes upregulated and 11 downregulated. In terms of a shared response between ARP23 MS and MC treatments, 8 genes were upregulated and 6 were downregulated in both treatments. Overall our results indicated that ARP23 mounts a different repertoire of DEGs in both MS and MC treatments (Table S2).

In terms of DEGs in the ARP23 MS and MC treatments. Only two common GO terms are overrepresented in the upregulated DEG lists, carbohydrate metabolic process (GO:0005975) and isomerase activity (GO:0016853). Interestingly many shared GO terms are overrepresented in the downregulated DEG lists relating to the negative regulation of processes including negative regulation of biosynthetic process (GO:0009890), negative regulation of metabolic process (GO:0009892), negative regulation of gene expression (GO:0010629) and negative regulation of cellular macromolecule biosynthetic process (GO:2000113) (Table S3). We also observed that the ARP23 MS treatment downregulates both intracellular protein transport (GO:0006886) and vesicle-mediated transport (GO:0016192) (Table S3).

3.5.4. Comparison of DEG profiles across strains and treatments

Comparisons between DEG profiles were made between each strain and each treatment (Figs. 5 and 6A). The highest number of unique DEGs per strain were in the A15 MS treatment in terms of upregulation ($n = 219$), the CWH MC treatment upregulation ($n = 57$) and downregulation in the MS treatment for ARP23 ($n = 296$). Our results indicate that *A. bisporus* demonstrates a strain-specific response to both early (MS) and late (MC) MVX-inoculation. The number of DEGs common to at least two strains is generally quite low (Fig. 6B). In terms of similarities between individual strains, the upregulated genes of A15 MS and ARP23 MS share the highest number between any pair-wise comparison ($n = 26$). The only incidence of commonality between all three strains is in the MS treatment with a single upregulated gene (accession:206844) of unknown function (Fig. 6B). All DEGs downregulated at MC are unique to each strain, suggesting MVX invokes strain-specific suppression of transcription.

Overall DEGs from all strains share a trend whereby the gene expression response to MVX was shown to be greater in mushrooms formed from mycelium exposed to MVX viruses at an earlier stage (MS treatments). A15 fruit bodies showed upregulation ($n = 304$) of a variety of genes when infected with MVX, whereas ARP23 primarily displayed repressed regulatory mechanisms of genes when MVX-infected ($n = 302$) (Fig. 5 and Table S2).

3.6. Proteomic response to MVX-inoculation in fruit bodies of A15, CWH and ARP23

We also examined the proteomic response of fruitbodies to MVX infection using LFQ proteomic analysis. In total 1,746, 1,607, 1777 proteins were located for the CWH, A15 and ARP23 strains (Fig. S1). Our results revealed significant differences in relative abundances and unique translation of proteins between fruit-bodies of non-infected (control), early (MS) and late (MC) infection treatments. Statistically significant differentially abundant (SSDA) proteins were evaluated for their possible role in relation to MVX-infection ($P < 0.05$, $\log_2$ fold change ± 1.0, −1.0). All SSDA proteins were tabulated for A15, CWH and ARP23 treatments (Table 1). A list of SSDA proteins in SCC and OWC can be viewed in supplementary information (Table S4).

3.6.1. A15 proteomic response

Of the 1607 proteins located for the three A15 treatments 1177 were common to all three. The A15 MS treatment contained 12 treatment specific proteins, while the MC treatment contained 152 treatment specific proteins (Table S5). Furthermore, the A15 MC & MS treatments contained 46 shared proteins not located in the control treatment (Fig. S1). An increase in abundance for three proteins in the A15 MS treatment were observed (mismatched base pair cruciform DNA recognition protein, an unknown protein and heterokaryon incompatibility protein Het-C). Three proteins also displayed increased abundance in the MC treatment (myo-inositol-1phosphate synthase, lectin, DAHP synthetase I family) (Table 1). Decreased abundance of four and five proteins were detected for MS and MC treatments respectively (Table 1). A number of the underabundant proteins were specific to fruit bodies, biosynthesis of polysaccharides and certain ribosomal proteins (Table 1). The greatest fold change of any SSDA protein was for a myo-inositol-1-phosphate synthase in the A15 MC treatment compared to control ($\log_2$ 3.93-fold; Table 1). Another protein with increased abundance in the A15 MC treatment is lectin. There are no shared over/underabundant proteins between the A15 MS and MC treatments (Table 1).

3.6.2. CWH proteomic response

Of the 1746 proteins located for the CWH treatments 1289 were common to all three treatments (control, MC and MS). The CWH MS treatment contained 157 unique proteins, while the CWH MC treatment contained 33 (Table S5). Furthermore, the CWH MC & MS treatments contained 66 shared proteins not located in the control treatment (Fig. S1). Increased abundance in the CWH strain was limited to a single protein in the MS treatment (GHMP kinases, Table 1). Decreased abundance was observed for nine proteins in the MS treatment and a single protein in the MC treatment (Table 1). There are no shared over/underabundant proteins between the CWH MS and MC treatments.

3.6.3. ARP23 proteomic response

Of the 1777 proteins located for the three ARP23 treatments, 961 were common to all three. The MS treatment contained no treatment specific proteins, while the MC treatment contained 93 treatment specific proteins. Interestingly, the ARP23 MC & MS treatments contained 720 shared proteins not located in the control treatment (Fig. S1). A different pattern of protein abundance was found in SSDAs of ARP23. Relative to A15 and CWH, increased abundance of SSDA proteins was greater for ARP23 MS (16 proteins) and MC (15 proteins) (Table 1). The highest and third highest fold-change ($\log_2$ 4.45-fold and $\log_2$ 2.14-fold, respectively) in the ARP23 MC treatment was for a protein containing an EF-hand domain involved in calcium ion binding (Table 1). EF-hand domain and calcium signalling are well known co-ordinators in response to biotic and abiotic stress stimuli (Day et al., 2002). Both ARP23 MS and MC treatments show an increase in abundance for a protein annotated as belonging to the DJ-1/PfpI family (Table 1).

4. Discussion

In this study, a model system was established to study a fungal–mycoviral interaction in a semi commercial-scale crop.

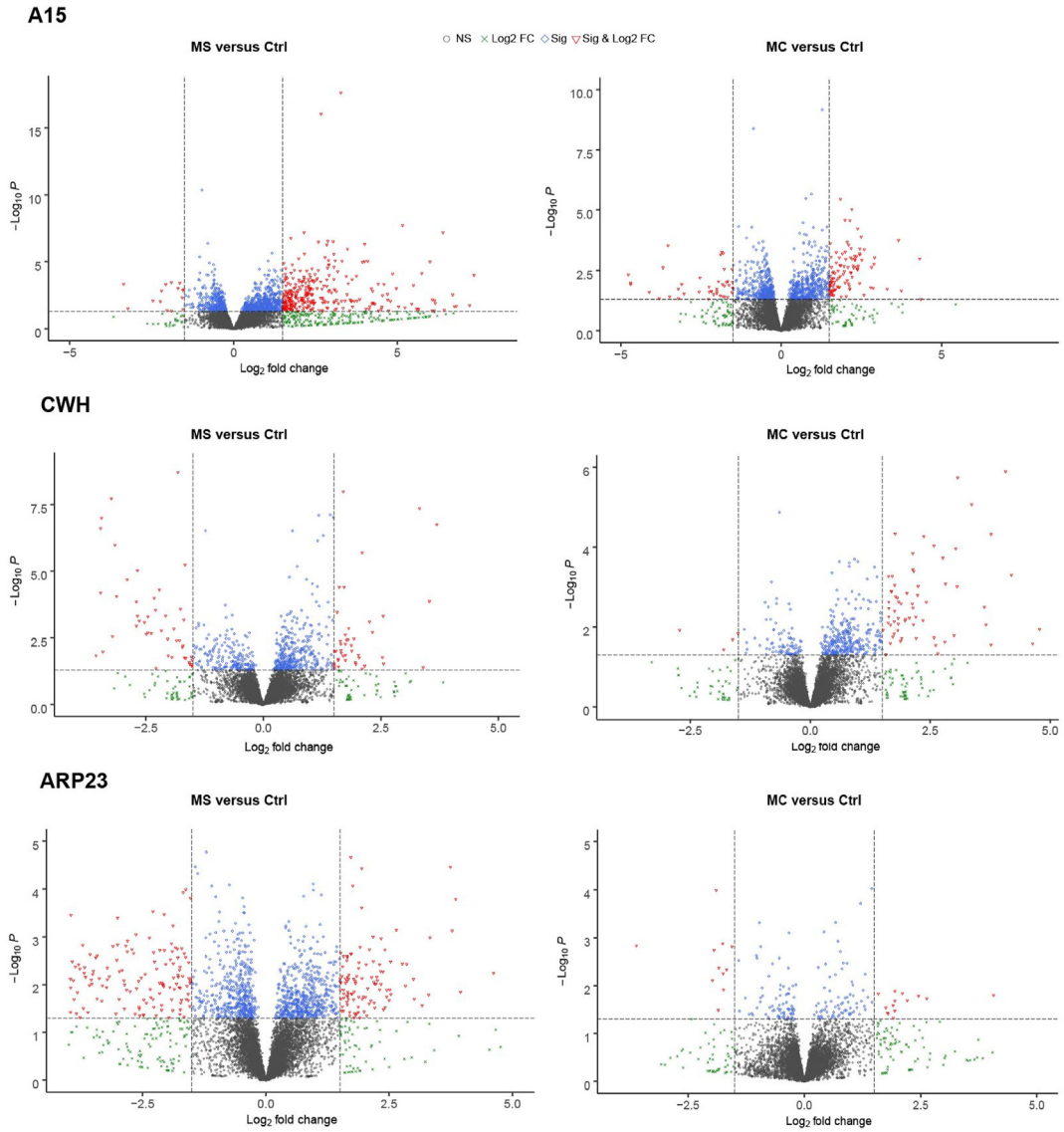

Fig. 5. DEGs of strains A15, CWH and ARP23 for MS (early MVX inoculation) and MC (late MVX inoculation) treatments compared to non-inoculated control mushrooms. Values above the horizontal dotted line represent $P < 0.05$ and the values the left and to the right of the vertical dotted lines represent Log_2 fold changes < -1.5 and >1.5, respectively.

Many studies focus on fungal–viral interactions in the context of the biocontrol of pathogenic fungi (Nuss 2005; Xie and Jiang 2014). Here, the interface of mycovirus and fungus is in the context of an economically important, globally cultivated food source. As such, the response of different strains of *A. bisporus* to MVX-inoculation was analysed through *in vitro* transmission assays in the mycelium, diagnostics of *in vivo* transmission to fruit bodies, fruit body transcriptomic characterisation of three - strains and fruit body proteomics of five strains.

Mycoviruses are intracellular with little documented extracellular route of transmission. Instead, vectors of mycoviral infection consist of systems of vertical and horizontal transmission (Pearson et al., 2009). In Basidiomycete fungi, vertical transmission refers to the release of spores from the basidia of virus-infected fruit bodies harbouring viruses/virus elements as noted, for example, in La France Isometric virus (Romaine et al., 1993). Horizontal transmission involves the transfer of viruses via anastomosis between infected and non-infected mycelia, the primary mode of transmission of MVX (Grogan et al., 2003). The transmission potential of MVX was investigated *in vitro* over a time-course totalling 12 days from initial anastomosis of a donor strain (MVX-1153) to a variety of five different acceptor strains (Fig. 1A). MVX-1153 was isolated from an A15 commercial crop and so exhibits full vegetative compatibility with A15. In contrast, vegetative compatibility is visibly lower with the four other strains (Fig. 1B). Vegetative incompatibility is a known barrier to mycoviral transmission due to the inhibition of plasmogamy between differing hyphae (Kashif et al., 2019). The lack of interaction observed *in vitro* between the donor and four of the acceptors supports the hypothesis that MVX transmission will not occur between strains that are vegetatively incompatible in comparison to full transmission expected in A15. However our results detected AbV16 in all strains at each time-point, with the exception of SCC T2 (Fig. 1C). This suggests that there were sufficient interactions between hyphae of MVX-1153 and all five acceptor strains to facilitate the transfer of MVX-viruses to all strains. The findings from our *in vitro* transmission experiment suggests that a seemingly minimal level of interaction between infected and non-infected hyphae is enough for transmission of

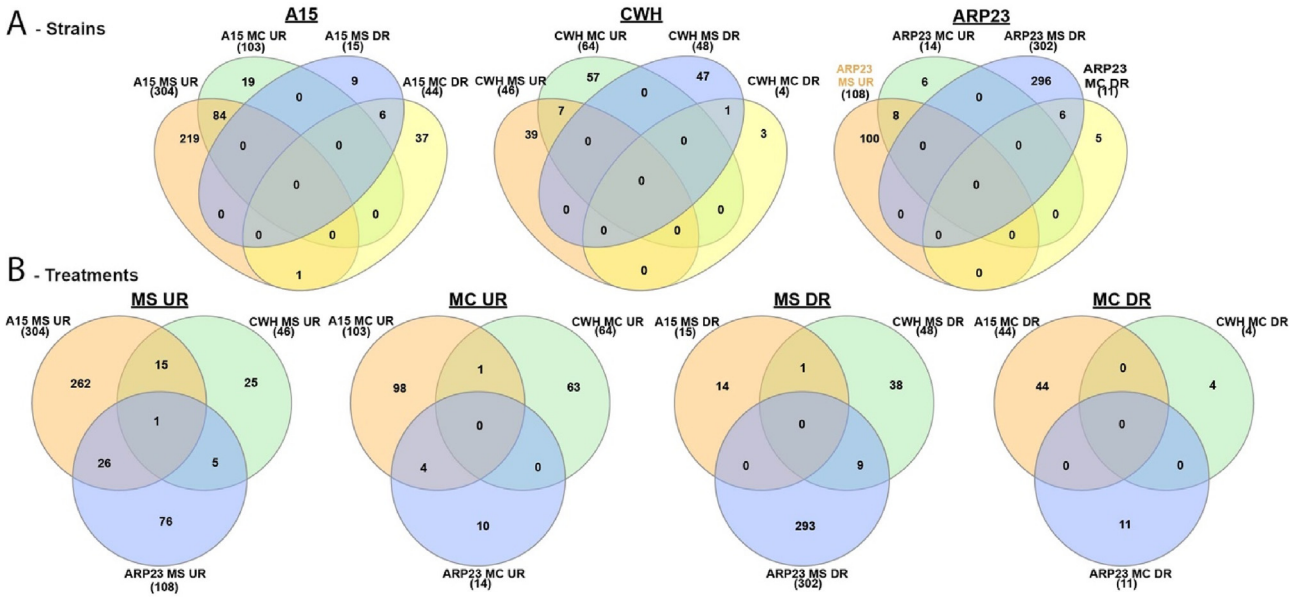

Fig. 6. Common and unique significantly DEGs in strains A15, CWH and ARP23 in each treatment. A: Four set Venn diagrams represent up-regulated (UR) and down-regulated (DR) genes for MS and MC treatments for a given strain. **B:** Three set Venn diagrams represent comparisons of the profiles of UR and DR DEGs by treatment. Almost no DEGs were common to any strain in any comparison.

MVX, even though the overall impression is that the strains are incompatible. *In vitro* transmission assays cannot replicate the complexity of the mycelial network formed within compost beds and studies have shown these types of experiments are not robust enough to draw firm conclusions on what might happen within complex biological systems and an experimental design closer to the biological system in which the mycoviruses occur *in vivo* is recommended (Brusini and Robin 2013).

MVX-diagnostics of fruit bodies from an *in vivo* infection experiment revealed differences in the detection of MVX transmission between different strains (Fig. 2). A15, as anticipated, showed the highest degree of AbV16 transmission and detection of any strain, with the MC treatment displaying positives in all replicates. SCC, OWC and ARP23 fruitbodies did not show presence of AbV16 in the MS treatment, but each showed detection in one out of three replicates in the MC treatment (Fig. 2). In contrast, only one AbV16-positive was detected in the CWH MS treatment, and none in the MC treatment. Based on the MVX frequency within the MC treatment, the results suggest that MVX transmission would appear to be more difficult at this time point. The finding of AbV6 in the ARP23 MS and MC treatments was unexpected (Fig. 2). The AbV6 virus is more associated with the bare patch disease phenotype and does not tend to co-occur with the brown disease phenotype (Grogan et al., 2003). As AbV6 was not detected in the control ARP23 fruit bodies, this suggests the introduction of the MVX inoculum is somehow responsible, even though MVX-1153 did not test positively for AbV6 (Fig. 2). However, recent research using fluorescence in situ hybridisation (FISH) to localise viruses within mycelium, detected low levels of AbV6 in MVX-1153 (O'Connor et al., 2020), which had not been detected by rtPCR. The fact that AbV6 was shown by FISH to be localised intensely at hyphal tips, where anastomosis occurs, suggests that this low level of AbV6 could be transferred from MVX-1153 into ARP23, or other strains, following anastomosis, but unlike the other strains tested, only ARP23 appears to have replicated the virus within its mycelium to a level that was then detectable in fruitbodies by the standard rtPCR diagnostic tests for this virus. The presence of small numbers of AbV6 has been shown in uninfected mushrooms using a next generation sequencing approach (Deakin et al., 2017), where variability in the virome of different mushroom samples was recorded, suggesting that there may be other factors influencing which viruses persist and replicate within the host.

The introduction of MVX inoculation to a crop has been previously shown to result in symptom expression in a crop, with later inoculations often leading to greater symptom expression (Grogan et al., 2003; Fleming-Archibald et al., 2015). This was also evident in the chromometric analysis of our experimental crop, where, apart from strain SCC, mushrooms from all other strains showed increased discoloration symptoms following inoculation, and which were sometimes more pronounced with the later infection timing (Fig. 3). This is also despite the fact that the AbV16 virus was only detected in very few samples. The effect of MVX-1153 inoculum on the colour of ARP23 was not anticipated, as this is already a brown strain with average ΔE for the controls being between 45 and 50. This became significantly higher when the crop was exposed to MVX at either an early or late stage in the crop cycle indicating how quantitative colour measurement can be a useful diagnostic tool.

Yield data from experimental trials needs to be interpreted with caution due to the limitations of scale but nonetheless there was a clear difference in the yield of the five strains as anticipated, with the three most commercial strains yielding similarly. MVX infection has been shown to sometimes reduce yields (Grogan et al., 2003) but others (Fleming-Archibald et al., 2015) showed that yields following MVX infection with AbV16 could also be similar or slightly higher than controls. This adds a layer of complexity when studying MVX in commercial crops suggesting that viral infection may affect several attributes of the crop, not just phenotype.

The transcriptomic response of A15, CWH and ARP23 fruit bodies revealed highly distinct gene expression responses when crops were grown and inoculated with MVX. Different times of MVX inoculation revealed disparate regulation of genes in each strain (Fig. 6). Both A15 MS & MC treatments show reduced expression of genes involved in transporter activity (GO:0005215) and transmembrane transporter activity (GO:0022857). Additionally, the A15 MS treatment showed down-regulation of vesicle

Table 1
List of SSDA proteins from the proteomes of A15, CWH and ARP23 upon MVX-inoculations (MS and MC).

Strain	Treatment	Accession ID	Description	GO Description	Fold Change
A15	MS vs Ctrl	138343	*Mismatched base pair and cruciform DNA recognition protein*	No GO Terms	↑1.79
		184070	No annotation	No GO Terms	↑1.07
		225120	Heterokaryon incompatibility protein Het-C	No GO Terms	↑1.02
		194843	Ribosomal protein L1p/L10e family	No GO Terms	↓1.12
		193061	Fruit-body specific protein D	No GO Terms	↓1.14
		209431	Polysaccharide biosynthesis	No GO Terms	↓1.36
		190119	Glutathione S-transferase	Protein binding	↓1.45
	MC vs Ctrl	192199	Myo-inositol-1-phosphate synthase	Inositol biosynthetic process	↑3.93
		137962	Lectin	Carbohydrate binding	↑1.67
		138762	DAHP synthetase I family	Biosynthetic process	↑1.19
		208031	Oligosaccharyltransferase subunit Ribophorin II	Integral component of membrane	↓1.02
		195282	Glyoxal oxidase	No GO Terms	↓1.06
		205013	Serine aminopeptidase, S33	No GO Terms	↓1.33
		193429	Pro-kumamolisin activation	Serine-type endopeptidase activity	↓1.50
		195527	No annotation	No GO Terms	↓1.59
CWH	MS vs Ctrl	69119	GHMP kinases	ATP binding	↑1.05
		60502	Bromodomain - transcription regulation; WD domain	Nucleic acid binding	↓1.07
		196018	PTFIIS helical bundle-like domain	Nucleus	↓1.16
		192114	RNA recognition motif.	Nucleic acid binding	↓1.21
		189249	Ribosomal L28e protein family	No GO Terms	↓1.24
		138985	Ribosomal L38e protein family	Translation	↓1.50
		135521	Ribosomal protein L36e	Translation	↓1.70
		62224	NADH oxidase family	Oxidation-reduction process	↓2.19
		191532	Tyrosinase	Oxidoreductase activity	↓2.48
		137962	No annotation	No GO Terms	↓3.73
	MC vs Ctrl	193825	Fatty acid desaturase	Lipid metabolic process	↓1.04
ARP23	MS vs Ctrl	72787	Nucleotide triphosphate	ATP binding	↑3.12
		204794	RNA polymerase Rpb1	Transcription	↑2.44
		192204	DJ-1/Pfpl family	No GO Terms	↑1.98
		184646	Protein of unknown function DUF89	No GO Terms	↑1.96
		220287	Phospholipase	Catalytic activity	↑1.89
		191987	Chromosome region maintenance or exportin repeat	Nuclear export signal receptor activity	↑1.78
		150186	Dynamin	GTPase activity	↑1.57
		199569	Epimerase/dehydratase	Coenzyme binding	↑1.45
		179844	Thioredoxin	Cell redox homeostasis	↑1.44
		192046	Glucosyltransferase 24	Protein glycosylation	↑1.32
		199822	Ubiquitin-specific protease	Protein deubiquitination	↑1.20
		185821	Mur ligase	Biosynthetic process	↑1.14
		190804	PheRS DNA binding domain 3; tRNA synthetases class II core domain (F)	tRNA binding	↑1.02
		188389	Glutaminyl-tRNA synthetase	Nucleotide binding	↑1.05
		189443	Hexokinase	Carbohydrate metabolic process	↑1.06
		61271	zinc metalloprotease	No GO Terms	↑1.07
		215454	Amidohydrolase family	Hydrolase activity	↓1.12
		197323	Thi4 family	No GO Terms	↓1.81
	MC vs Ctrl	138931	EF-hand	Calcium ion binding	↑4.45
		147111	FAD binding domain	Oxidation-reduction process	↑2.23
		180834	EF-hand	Calcium ion binding	↑2.14
		121683	GMC oxidoreductase	Oxidation-reduction process	↑1.65
		192204	DJ-1/Pfpl family	No GO Terms	↑1.60
		193127	UBX domain	Protein binding	↑1.60
		143608	Carbohydrate kinase	ADP-dependent NAD(P)H-hydrate dehydratase activity	↑1.58
		132803	Predicted Protein	Hydrolase activity	↑1.49
		195174	Amidohydrolase	Hydrolase activity	↑1.44
		191253	TPR-like protein	Protein binding	↑1.40
		192618	No Pfam	No GO Terms	↑1.28
		217931	Domain of unknown function (DUF427)	No GO Terms	↑1.17
		145028	Cytochrome *b*5-like Heme/Steroid binding domain	No GO Terms	↑1.01
		205090	NADPH-dependent FMN reductase	Oxidoreductase activity	↑1.05
		139898	No Pfam	No GO Terms	↑1.09
		192925	Phosphoglycerate mutase-like protein	No GO Terms	↓1.16

transport (GO:0016192) (Table S3). Detailed information on where MVX localises in the cells of infected mycelium and fruit bodies, and how the virus moves from cell to cell, is lacking. However, it is hypothesised that vesicles and vesicle-transport are important for virus movement via virus packaging in membrane vesicles (Romaine et al., 1994). Our results suggest that when an A15 mushroom crop is infected it may attempt to curtail infection through downregulation of vesicle transporting activities.

DEGs of the CWH strain also show a lack of commonality between the two inoculation times (Fig. 6). Some of the highest transcript levels observed in the CWH MS treatments are related to antiviral proteins (accession: 195778). An autophagy related protein (accession: 146937) is also observed in CWH MS, autophagy is

known for its antiviral and proviral potential (Chiramel et al., 2013) (Table 1 and S2). Although, it is less likely that MVX elicits autophagy for proviral purposes, as this process is not upregulated in the more susceptible strain A15 Therefore, CWH may utilize this system as a mechanism for antiviral defence. Interestingly, downregulation of terms related to autophagy (GO:0006914 & GO:0061919) were enriched in the CWH MC treatment (Table S3), perhaps downregulation of these processes may reflect the 'aftermath' of MVX infection and return to cellular homeostasis in these fruit bodies. Although, further investigation is needed to test this hypothesis.

Early MVX-inoculation (MS) elicited a considerably larger transcriptomic response in ARP23 than the later inoculation (MC) (Fig. 6). A large variety of negative regulatory terms are down regulated in MS and MC of ARP23 (Table S3). Furthermore, GO enrichment analysis of ARP23 MS DEGs reveals downregulation of terms that would putatively inhibit viral transport and replication, such as mRNA processing (GO:0006397), protein maturation (GO:0051604), vesicle-mediated transport (GO:0016192) and gene expression (GO:0010467) (Table S3).

The proteomes of the five strains used in this study revealed an interesting clustering pattern with respect to the treatment of plots, where MS and MC treatments did not cluster, except in the case of the SCC strain (Fig. 7B). This hierarchical clustering suggests the proteomes of control uninfected and late MVX inoculation (of which four out of the five strains contain at least one MVX-infected replicate) are more similar than the earlier MVX-inoculation. This may show how responsive genes are not induced as highly as those in MS treatments, reflecting the greater impact of later infections on crops and the important role played by the mycelium in terms of the fruit bodies outcome to infection. We cross checked all proteins that were present in either the MS and MC treatment for each strain but absent in the corresponding control strains. Interestingly only a single protein related to autophagy (accession:195614) was located. Autophagy related genes were also located in the DEGs of the CWH MS treatment and as previously mentioned autophagy is known for its antiviral and proviral potential (Chiramel et al., 2013). Of the SSDA proteins, the greatest fold change was for a myo-inositol-1-phosphate synthase in A15 MC compared to control (log_2 3.93-fold; Table 1). Myo-inositol-1-phosphate synthase catalyses the biosynthesis of inositol, essential precursors of structures integral to lipid membrane (Lohia et al., 1999). Many roles are attributed to inositol phosphates including cytoskeletal architecture organisation, control of membrane trafficking, regulation of gene expression and mRNA export (York et al., 2001). Previous studies examined the metabolome of commercial white mushrooms upon mechanical damage-induced browning (O'Gorman et al., 2012). Myo-inositol was identified as one of the most important markers in post-harvest mechanical damage (O'Gorman et al., 2012). This may provide evidence for a correlation between the browning ensued by mechanical damage and the browning disease phenotype induced by MVX, through biosynthesis of myo-inositol. Also high in abundance in the A15 MC treatment is lectin (Table 1). The range of processes known for fungal lectins are unclear. Certain lectins are known for their defence-response roles, though characterisation of these defences is limited (Bleuler-Martinez et al., 2017; Tayyrov et al., 2018). SSDA of a mismatched base pair and cruciform DNA recognition protein was also detected in the A15 MS treatment (also present as a DEG in the ARP23 MS treatment). Detailed functional characterisation of this protein is limited except that it contains a

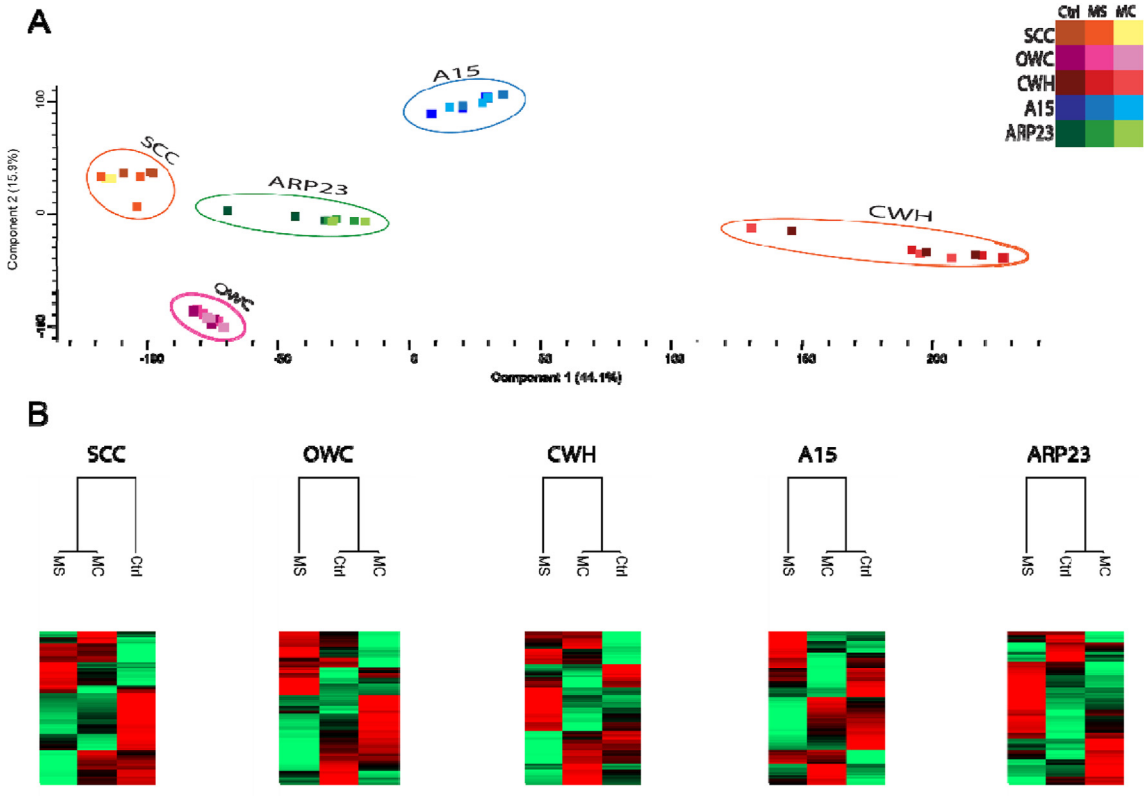

Fig. 7. Clustering analysis of the proteomes of five strains *A. bisporus* control (Ctrl), MVX-inoculation at the beginning of spawn run (MS), MVX-inoculation at the beginning of case run (MC). (A) Principal component analysis shows the grouping of each strain. (B) Hierarchical clustering of the proteomes of each strain where relative protein expression is shown in heat maps, high abundance is represented by red, average abundance by black and low abundance by green. (For interpretation of the references to colour in this figure legend, the reader is referred to the Web version of this article.)

Pfam domain for csbd-like (PF05532). Csbd-like protein is known in bacteria for its role in stress response (Prágai and Harwood 2002). Abundance of ribosomal proteins is significantly lower in A15 MS and CWH MS treatments, whereas no SSDA ribosomes are evident in MVX-inoculated ARP23 groups (Table 1). Viruses are well known for their capacity to recruit host ribosomes for viral protein biosynthesis and so a host response may lead to inhibition of ribosomal activity to curtail virus replication (Li 2019). CWH MS also reveals low levels of SSDA proteins of three transcription factor/DNA binding proteins (Table 1). This suggests that CWH represses translation of proteins that may be otherwise commandeered by MVX. The SSDA proteins in the proteomes of ARP23 MS and MC consisted of high abundance SSDAs over low abundance for an array of proteins (Table 1). The biological processes of these proteins vary from nucleotide binding, post-translational modifications, nuclear exportation activities, transcription and carbohydrate metabolism (Table 1).

5. Conclusion

This work has demonstrated that a variety of strains of *A. bisporus* can become infected by the causal virus for brown cap disease phenotypes through early interaction/anastomosis with MVX-infected mycelium. Infection impacts fruit bodies by altering yields, producing abnormal phenotypes and causing browning of fruit bodies to occur. AbV16 is detected at different frequencies in fruit bodies depending on strain susceptibility and the timing of inoculation, where introducing MVX closer to primordia formation (pinning) results in more disease symptoms. MVX induces distinct transcriptomic and proteomic responses between strains and point of inoculation. Of the strains tested, A15 is most susceptible to infection, likely due to the its vegetative compatibility with the commercial sources of MVX inoculum. This is reflected in cellular stress responses and putative mechanical damage via myo-inositol biosynthesis. CWH fruit bodies are less susceptible to MVX and demonstrated a variety of antiviral activity when AbV16 was detected, including high levels of ribonucleases and autophagy. CWH fruit bodies testing negative for MVX still showed evidence of viral activity, possibly indicating eradication of viruses over the prevention of initial entry from the mycelium. ARP23, though almost as unsusceptible to MVX as CWH, mounted an entirely different transcriptomic and proteomic response. This could be due in part to detectable levels of AbV6 in ARP23 fruit bodies. Antiviral strategies of this strain amounted to downregulation of a plethora of processes, namely gene expression. This work details the host response from fruit bodies of a variety of *A. bisporus* strains to MVX-inoculation. This work will add to our understanding of the how MVX impacts the fruit bodies of *A. bisporus* and the processes mounted by host and induced by pathogen.

Acknowledgments

EOC was funded by a Teagasc Walsh Scholarship (grant reference number 10564231). Mass spectrometry facilities were funded by Science Foundation Ireland (SFI 12/RI/2346(3)).

Appendix A. Supplementary data

Supplementary data to this article can be found online at https://doi.org/10.1016/j.funbio.2021.04.005.

References

Altschul, S.F., Madden, T.L., Schäffer, A.A., Zhang, J., Zhang, Z., Miller, W., Lipman, D.J., 1997. Gapped BLAST and PSI-BLAST: a new generation of protein database search programs. Nucleic Acids Res. 25 (17), 3389–3402.
Bleuler-Martinez, S., Stutz, K., Sieber, R., Collot, M., Mallet, J.-M., Hengartner, M., Schubert, M., Varrot, A., Künzler, M., 2017. Dimerization of the fungal defense lectin CCL2 is essential for its toxicity against nematodes. Glycobiology 27 (5), 486–500.
Brusini, J., Robin, C., 2013. Mycovirus transmission revisited by in situ pairings of vegetatively incompatible isolates of *Cryphonectria parasitica*. J. Virol. Methods 187 (2), 435–442.
Chiramel, A., Brady, N., Bartenschlager, R., 2013. Divergent roles of autophagy in virus infection. Cells 2 (1), 83–104.
Conesa, A., Gotz, S., Garcia-Gomez, J.M., Terol, J., Talon, M., Robles, M., 2005. Blast2GO: a universal tool for annotation, visualization and analysis in functional genomics research. Bioinformatics 21 (18), 3674–3676.
Cox, J., Mann, M., 2008. MaxQuant enables high peptide identification rates, individualized p.p.b.-range mass accuracies and proteome-wide protein quantification. Nat. Biotechnol. 26 (12), 1367–1372.
Day, I.S., Reddy, V.S., Shad Ali, G., Reddy, A.S.N., 2002. Analysis of EF-hand-containing proteins in *Arabidopsis*. Genome Biol. 3 (10). RESEARCH0056.
Deakin, G., Dobbs, E., Bennett, J.M., Jones, I.M., Grogan, H.M., Burton, K.S., 2017. Multiple viral infections in *Agaricus bisporus* - characterisation of 18 unique RNA viruses and 8 ORFans identified by deep sequencing. Sci. Rep. 7 (1), 2469.
Eastwood, D., Green, J., Grogan, H., Burton, K., 2015. Viral agents causing Brown cap mushroom disease of *Agaricus bisporus*.Cullen D, editor. Appl. Environ. Microbiol. 81 (20), 7125–7134.
Fleming-Archibald, C., Ruggiero, A., Grogan, H.M., 2015. Brown mushroom symptom expression following infection of an *Agaricus bisporus* crop with MVX associated dsRNAs. Fungal Biol. 119 (12), 1237–1245.
Gaze, R.H., Calvo-Bado, L., Challen, M.P., Adie, B.A.T., Romaine, C.P., 2000. A new virus disease of *Agaricus bisporus*? Mushroom Sci. 15, 701–705.
Gilmer, D., Ratti, C., 2017. ICTV virus taxonomy profile: Benyviridae. J. Gen. Virol. 98 (7), 1571–1572.
Gotz, S., Garcia-Gomez, J.M., Terol, J., Williams, T.D., Nagaraj, S.H., Nueda, M.J., Robles, M., Talon, M., Dopazo, J., Conesa, A., 2008. High-throughput functional annotation and data mining with the Blast2GO suite. Nucleic Acids Res. 36 (10), 3420–3435.
Grogan, H.M., Adie, B.A.T., Gaze, R.H., Challen, M.P., Mills, P.R., 2003. Double-stranded RNA elements associated with the MVX disease of *Agaricus bisporus*. Mycol. Res. 107 (2), 147–154.
Jones, P., Binns, D., Chang, H.-Y., Fraser, M., Li, W., McAnulla, C., McWilliam, H., Maslen, J., Mitchell, A., Nuka, G., et al., 2014. InterProScan 5: genome-scale protein function classification. Bioinformatics 30 (9), 1236–1240.
Kashif, M., Jurvansuu, J., Vainio, E.J., Hantula, J., 2019. Alphapartitiviruses of heterobasidion wood decay fungi affect each other's transmission and host growth. Front Cell Infect Microbiol. 9.
Kim, D., Langmead, B., Salzberg, S.L., 2015. HISAT: a fast spliced aligner with low memory requirements. Nat. Methods 12 (4), 357–360.
Kim, J.-M., Yun, S.-H., Park, S.-M., Ko, H.-G., Kim, D.-H., 2013. Occurrence of dsRNA mycovirus (LeV-FMRI0339) in the edible mushroom *Lentinula edodes* and meiotic stability of LeV-FMRI0339 among monokaryotic progeny. Plant Pathol. J. 29 (4), 460–464.
Kim, S.-W., Kim, M.-G., Kim, J., Lee, H.-S., Ro, H.-S., 2008. Detection of the mycovirus OMSV in the edible mushroom, *Pleurotus ostreatus*, using an SPR biosensor chip. J. Virol. Methods 148 (1–2), 120–124.
Li, S., 2019. Regulation of ribosomal proteins on viral infection. Cells 8 (5), 508.
Lohia, A.C., Hait, N., Lahiri Majumder, A., 1999. l-myo-Inositol 1-phosphate synthase from *Entamoeba histolytica*. Mol. Biochem. Parasitol. 98 (1), 67–79.
Love, M.I., Huber, W., Anders, S., 2014. Moderated estimation of fold change and dispersion for RNA-seq data with DESeq2. Genome Biol. 15 (12), 550.
Magae, Y., 2012. Molecular characterization of a novel mycovirus in the cultivated mushroom, *Lentinula edodes*. Virol. J. 9 (1), 60.
Magae, Y., Sunagawa, M., 2010. Characterization of a mycovirus associated with the brown discoloration of edible mushroom, *Flammulina velutipes*. Virol. J. 7 (1), 342.
Martin, M., 2011. Cutadapt removes adapter sequences from high-throughput sequencing reads. EMBnet J. 17 (1), 10.
Morin, E., Kohler, A., Baker, A.R., Foulongne-Oriol, M., Lombard, V., Nagye, L.G., Ohm, R.A., Patyshakuliyeva, A., Brun, A., Aerts, A.L., et al., 2012. Genome sequence of the button mushroom *Agaricus bisporus* reveals mechanisms governing adaptation to a humic-rich ecological niche. Proc. Natl. Acad. Sci. Unit. States Am. 109 (43), 17501–17506.
Nuss, D.L., 2005. Hypovirulence: mycoviruses at the fungal–plant interface. Nat. Rev. Microbiol. 3 (8), 632–642.
O'Connor, E., Coates, C.J., Eastwood, D.C., Fitzpatrick, D.A., Grogan, H., 2020. FISHing in fungi: visualisation of mushroom virus X in the mycelium of *Agaricus bisporus* by fluorescence in situ hybridisation. J. Microbiol. Methods 173, 105913.
O'Gorman, A., Barry-Ryan, C., Frias, J.M., 2012. Evaluation and identification of markers of damage in mushrooms (*Agaricus bisporus*) postharvest using a GC/MS metabolic profiling approach. Metabolomics 8 (1), 120–132.
O'Keeffe, G., Hammel, S., Owens, R.A., Keane, T.M., Fitzpatrick, D.A., Jones, G.W., Doyle, S., 2014. RNA-seq reveals the pan-transcriptomic impact of attenuating

the gliotoxin self-protection mechanism in *Aspergillus fumigatus*. BMC Genom. 15 (3), 894.
Owens, R.A., O'Keeffe, G., Smith, E.B., Dolan, S.K., Hammel, S., Sheridan, K.J., Fitzpatrick, D.A., Keane, T.M., Jones, G.W., Doyle, S., 2015. Interplay between gliotoxin resistance, secretion, and the methyl/methionine cycle in *Aspergillus fumigatus*. Eukaryot. Cell 14 (9), 941–957.
Patro, R., Duggal, G., Love, M.I., Irizarry, R.A., Kingsford, C., 2017. Salmon provides fast and bias-aware quantification of transcript expression. Nat. Methods 14 (4), 417–419.
Pearson, M.N., Beever, R.E., Boine, B., Arthur, K., 2009. Mycoviruses of filamentous fungi and their relevance to plant pathology. Mol. Plant Pathol. 10 (1), 115–128.
Prágai, Z., Harwood, C.R., 2002. Regulatory interactions between the Pho and σB-dependent general stress regulons of *Bacillus subtilis*. Microbiology 148 (5), 1593–1602.
Romaine, C.P., Schlagnhaufer, B., Goodin, M.M., 1994. Vesicle-associated double-stranded ribonucleic acid genetic elements in *Agaricus bisporus*. Curr. Genet. 25 (2), 128–134.
Romaine, C.P., Ulhrich, P., Schlagnhaufer, B., 1993. Transmission of La France isometric virus during basidiosporogenesis in *Agaricus bisporus*. Mycologia 85 (2), 175.
Sonnenberg, A.S.M., Baars, J.J.P., Gao, W., Visser, R.G.F., 2017. Developments in breeding of *Agaricus bisporus* var. *bisporus*: progress made and technical and legal hurdles to take. Appl. Microbiol. Biotechnol. 101 (5), 1819–1829.
Suzuki, N., Ghabrial, S.A., Kim, K.-H., Pearson, M., Marzano, S.-Y.L., Yaegashi, H., Xie, J., Guo, L., Kondo, H., Koloniuk, I., Hillman, B.I., 2018. ICTV virus taxonomy profile: Hypoviridae. J. Gen. Virol. 99 (5), 615–616.
Tayyrov, A., Schmieder, S.S., Bleuler-Martinez, S., Plaza, D.F., Künzler, M., 2018. Toxicity of potential fungal defense proteins towards the fungivorous nematodes *Aphelenchus avenae* and *Bursaphelenchus okinawaensis*.Drake HL. Appl. Environ. Microbiol. 84 (23).
Tyanova, S., Temu, T., Sinitcyn, P., Carlson, A., Hein, M.Y., Geiger, T., Mann, M., Cox, J., 2016. The Perseus computational platform for comprehensive analysis of (prote)omics data. Nat. Methods 13 (9), 731–740.
Xie, J., Jiang, D., 2014. New insights into mycoviruses and exploration for the biological control of crop fungal diseases. Annu. Rev. Phytopathol. 52 (1), 45–68.
York, J.D., Guo, S., Odom, A.R., Spiegelberg, B.D., Stolz, L.E., 2001. An expanded view of inositol signaling. Adv. Enzym. Regul. 41 (1), 57–71.
Yu, X., Li, B., Fu, Y., Jiang, D., Ghabrial, S.A., Li, G., Peng, Y., Xie, J., Cheng, J., Huang, J., Yi, X., 2010. A geminivirus-related DNA mycovirus that confers hypovirulence to a plant pathogenic fungus. Proc. Natl. Acad. Sci. Unit. States Am. 107 (18), 8387–8392.